Materials and Design xxx (2015) xxx

Contents lists available at ScienceDirect

Materials and Design

journal homepage: www.elsevier.com/locate/jmad

Graphical abstract

pp. xxx–xxx

Neat and GNPs loaded natural rubber fibers by electrospinning: Manufacturing and characterization

Ilaria Cacciotti*, John N. House, Claudia Mazzuca, Manlio Valentini, Francesco Madau, Antonio Palleschi, Paolo Straffi, Francesca Nanni

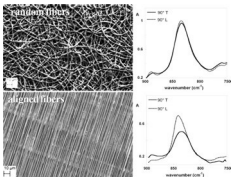

SEM micrographs and ATR spectra of random and aligned NR based fibers.

http://dx.doi.org/10.1016/j.matdes.2015.09.054
0264-1275/

Please cite this article as: I. Cacciotti, et al., Neat and GNPs loaded natural rubber fibers by electrospinning: Manufacturing and characterization, Materials and Design (2015), http://dx.doi.org/10.1016/j.matdes.2015.09.054

Materials and Design xxx (2015) xxx

Contents lists available at ScienceDirect

Materials and Design

journal homepage: www.elsevier.com/locate/jmad

Highlights

Materials and Design xxx (2015) xxx–xxx

Neat and GNPs loaded natural rubber fibers by electrospinning: Manufacturing and characterization

Ilaria Cacciotti[a,b,*], John N. House[c], Claudia Mazzuca[d], Manlio Valentini[b,e], Francesco Madau[b,e], Antonio Palleschi[d], Paolo Straffi[c], Francesca Nanni[b,e]

[a] *University of Rome "Niccolò Cusano", ~~INSTM RU,~~ Via Don Carlo Gnocchi 3, 00166 Rome, Italy*
[b] *Italian Interuniversity Consortium on Materials Science and Technology (INSTM), Italy*
[c] *Bridgestone Technical Center Europe, via Fosso del Salceto 13-15, 00128 Castel Romano (Rome), Italy*
[d] *University of Rome "Tor Vergata", Department of Chemical Science and Technology, Via della Ricerca Scientifica 1, 00133 Rome, Italy*
[e] *University of Rome "Tor Vergata", Department of Enterprise Engineering, Via del Politecnico 1, 00133 Rome, Italy*

- Natural rubber (NR) fibrous mats loaded with graphene nanoplatelets were successfully fabricated by electrospinning technique.
- It has been demonstrated that the electrospinning process is able to induce a strong orientation of the polymeric chains.
- The aligned fibers presented remarkably higher dichroic ratio values with respect to the randomly oriented ones.

http://dx.doi.org/10.1016/j.matdes.2015.09.054
0264-1275/

Materials and Design xxx (2015) xxx–xxx

Contents lists available at ScienceDirect

Materials and Design

journal homepage: www.elsevier.com/locate/jmad

Neat and GNPs loaded natural rubber fibers by electrospinning: Manufacturing and characterization

Ilaria Cacciotti [a,b,*], John N. House [c], Claudia Mazzuca [d], Manlio Valentini [b,e], Francesco Madau [b,e], Antonio Palleschi [d], Paolo Straffi [c], Francesca Nanni [b,e]

[a] University of Rome "Niccolò Cusano", ~~INSTM RU,~~ Via Don Carlo Gnocchi 3, 00166 Rome, Italy
[b] Italian Interuniversity Consortium on Materials Science and Technology (INSTM), Italy
[c] Bridgestone Technical Center Europe, via Fosso del Salceto 13-15, 00128 Castel Romano (Rome), Italy
[d] University of Rome "Tor Vergata", Department of Chemical Science and Technology, Via della Ricerca Scientifica 1, 00133 Rome, Italy
[e] University of Rome "Tor Vergata", Department of Enterprise Engineering, Via del Politecnico 1, 00133 Rome, Italy

ARTICLE INFO

Article history:
Received 6 May 2015
Received in revised form 10 August 2015
Accepted 10 September 2015
Available online xxxx

Keywords:
Natural rubber
Graphene nanoplatelets
Fibers
Films
Electrospinning
FTIR (polarized ATR)

ABSTRACT

The interest towards natural rubber (NR) is progressively increasing due to its sustainable production and remarkable mechanical properties, presenting a wide application range in the automotive industry and civil engineering. In this paper we report, for the first time, the use of electrospinning technique to produce neat and graphene nanoplatelets (GNPs, 1 wt.%) loaded natural rubber fibers. Both randomly distributed and aligned fibers (average diameter size ~1 μm) mats were obtained, resulting uniform and defect-free. A detailed characterization of these fibers is reported, including field emission-scanning electron microscopy (FEG-SEM), X-Ray diffraction (XRD) and infrared spectroscopy (FTIR-ATR) techniques. It has been demonstrated that the electrospinning process is able to induce a strong orientation of the polymeric chains in the case of aligned fibers, with respect to the randomly oriented fibers and solvent cast films.

1. Introduction

Among the fiber production techniques, electrospinning is a user friendly, versatile and low-cost method, which allows to manufacture different materials (e.g. polymers, ceramics, metals, composites) with diameters ranging from nanometers to micrometers and large surface area-to-volume ratio [1–6]. Only few attempts of electrospinning elastomers/rubbers are currently reported in literature, due to their poor spinning ability in conventional solvent systems, which is related to their viscoelastic behavior at room temperature and fiber formation mechanism during electrospinning. For example, only fibers based on polybutadiene rubber (BR) [7–8], synthethic cis-1,4-polyisoprene [9], blends of natural rubber (NR)/acrylonitrile butadiene styrene (ABS) [10] and of NR/polycaprolactone (PCL) [11] were successfully obtained by electrospinning technique. To the best of our knowledge, actually none of the papers reported in literature deals with sole natural rubber.

Among the elastomers, natural rubber attracts a lot of attention, due to its outstanding performance properties such as high elasticity, resilience and good fatigue resistance [12] and its application for the manufacture of more than 40,000 consumer products, including tires, wires, latex products, footwear, medical devices and sport components [13, 14]. In this framework, the present work reported a first attempt to develop neat and graphene nanoplatelets (GNPs) loaded natural rubber fibers by this technique. The application of electrospinning ~~technique~~ to ~~produce~~ natural rubber based fibers was achieved using the dry rubber (DR) extracted from natural rubber latex (NRL). The extracted DR was dissolved in chloroform to enhance its spinning ability. The GNPs were chosen and selected as conductive fillers in order to evaluate their influence on the microstructure of the obtained fibrous membranes. In this contest, several micro- and nano-sized conductive fillers, such as carbon black (CB), metallic powders (e.g. silver and copper), and carbon nanotubes (CNTs), are commonly used due to their light weight, high flexibility and ability to absorb mechanical shocks in order to prepare natural rubber composites [15], for applications in the fields of electromagnetic interference shielding, self-regulated heating, package material and pressure sensors [16]. It has been demonstrated that the filler properties, in terms of particle size, surface area, aggregate structure, surface activity and conductivity, can strongly influence the characteristics of the final composite [15]. The electrospinning set-up to produce both randomly distributed and aligned fibers was accomplished by properly tuning process parameters, in terms of applied voltage, needle–target distance, collector type (i.e. fixed or rotating, respectively). Furthermore, the crystallization and/or macromolecular orientation of the natural rubber chains in the produced randomly distributed and

* Corresponding author at: University of Rome "Niccolò Cusano", ~~INSTM RU,~~ Via Don Carlo Gnocchi 3, 00166 Rome, Italy.
E-mail address: ilaria.cacciotti@unicusano.it (I. Cacciotti).

http://dx.doi.org/10.1016/j.matdes.2015.09.054
0264-1275/

aligned fibers were investigated. Morphology thermal behavior, microstructure and the orientation of the polymeric chains were investigated by scanning electron microscopy (FEG-SEM), simultaneous thermogravimetric and differential analyses (TG-DTA), X-Ray diffraction (XRD) and infrared spectroscopy (ATR-IR), respectively.

2. Experimental

2.1. Preparation of dry rubber based solutions and suspensions

The natural rubber latex (*R1 International PTE LTD*) consisted in a colloidal suspension of cis-polyisoprene in natural rubber serum preserved with ca. 0.7% of ammonia and a mixture of lauric acid, tetramethyl thiuram disulfide and zinc oxide. The pH value of the suspension was 10 and the density at 20 °C of 0.998 g/cm^3. Firstly the latex was poured in a Petri dish and afterwards completely covered with acetone (*Carlo Erba Reagents*), in order to favor the evaporation of the emulsion's volatile components. This process was carried out until the final weight of the compound was 40% less than the initial weight (i.e. dry rubber). The obtained DR was then dissolved in chloroform ($CHCl_3$, 99%, *Carlo Erba Reagents*) at 1 and 2% *w/w* under constant magnetic stirring for three days. Hybrid suspensions based on rubber and graphene nanoplatelets (GNPs, *Cometox*, average thickness 15 nm, typical surface area 50 ÷ 80 m^2/g, as reported in the datasheet) were also prepared. The GNPs dispersion was performed in chloroform by sonication (*Sonics Vibracell CV33*) for 1 h at 30% amplitude in an ice bath, followed by centrifugation (Thermo Electron Corporation ALC 4218) for 1 h at 3000 rpm and further sonication for 1 h at 30% amplitude. Afterwards, the dry rubber was added to the GNPs suspension in order to obtain a 2% *w/w* rubber concentration in chloroform and a 1% *w/w* concentration of GNPs compared to the dry latex content. The viscosity of the as received latex and all the prepared solutions/suspensions was measured at 25 °C using a dynamic viscometer (*Brookfield DV-II+*, Middleboro, MA, USA), equipped with a SC4-21 spindle, and the conductivity measurements of the different samples were carried out with an electrical conductimeter (CDM230, *Analitica De Mori*, Italy).

2.2. Fabrication of neat and hybrid fibrous mats by electrospinning

The prepared solutions and suspensions were poured in a glass syringe (*Socorex*, Switzerland) equipped with a 20 G needle, fixed in a digitally controlled syringe pump (*KD Scientific*, MA, USA) and electrospun in air at room temperature in the following conditions: applied voltage 16 kV, feed rate 0.5 ml/h, needle–target (N–T) distance 10–18 cm and 12–16 cm for fixed and rotating targets, respectively. In Table 1 the samples designation and the related electrospinning parameters are summarized. Finally, as reference, neat and hybrid films were prepared by solvent casting technique, pouring the prepared solutions/suspensions in Petri dishes and left to dry under the fume hood until the solvent was completely evaporated. Furthermore the same procedure was adopted to prepare neat latex films starting from the as-purchased solution, with and without the acetone addition (i.e. dry rubber w acetone and dry rubber w/o acetone, respectively).

2.3. Characterization of neat and hybrid fibrous mats by electrospinning

The morphology of all samples was investigated by means of Scanning Electron Microscopy (FEG-SEM, *Cambridge Leo Supra 35*). The average fiber size was determined from SEM micrographs by means of Image J (NIH) software. X-ray diffraction analyses (XRD, *Philips X'Pert*) were performed in the following conditions: CuKα λ = 1.5402 Å, 2θ range 5°–90°, step size 0.020°, time per step 2 s. Thermogravimetric measurements (TG-DTA) were carried out in nitrogen atmosphere (flow 80 cm^3/min) by simultaneous thermogravimetric and differential thermal analysis (TG-DTA, *Netzsch STA 409*), in the following conditions: sample weight about 60 mg, temperature range 20–1250 °C, heating rate 5 °C/min. In order to characterize the natural rubber components, FTIR spectra were acquired on a *Thermo-Nicolet* (mod. Nexus 670) instrument (*Thermo Scientific Inc.*, Madison WI), equipped with an attenuated total reflectance (ATR) ZnSe cell for measurement in the 4000–750 cm^{-1} region, at a resolution of 4 cm^{-1}. Spectra were collected by placing and pressing the samples into contact with the ATR cell. A total of 256 scans were collected for each sample. In addition, polarized ATR-IR spectra were acquired on all samples in order to study the molecular orientation of polymer chains due to the polymer processing technique. To achieve a complete analysis of the samples, four separate spectra were acquired using polarized light at 0° and 90° with respect to the sample's plane and positioning the samples longitudinally (L) and transversally (T) to the direction of the stress applied during the processing. Thus the dichroic ratio was evaluated by the ratio between peak intensities in two different configurations, as expressed with the followings equations:

$$R_X\left(\frac{\alpha}{\beta}\right) = \left(\frac{A(\alpha)}{A(\beta)}\right)_X \quad (1)$$

$$R_\alpha\left(\frac{X}{Y}\right) = \left(\frac{A(X)}{A(Y)}\right)_\alpha \quad (2)$$

where X and Y are the longitudinal and transversal configurations and α and β the polarizer orientations [17]. In all cases the peak at 2960 cm^{-1}, related to the CH_3 asymmetric stretching, was used as non-dichroic peak (i.e. as reference), since it presents a unitary dichroic ratio independently of the polymer structure. While the peaks at 1367 cm^{-1} (CH_3 deformation) and at 837 cm^{-1} (=CH out of plane bending) were selected to calculate the dichroic ratio (R) in all the selected configurations, in order to investigate the orientation of the macromolecular chains of the cis-1,4-polyisoprene [18,19].

Table 1
Designation of the electrospun neat and hybrid fibers and used process parameters (all the samples were electrospun using a feed rate of 0.5 ml/h and a voltage of 16 kV).

Sample	Latex concentration (wt.%)	GNPs filler concentration (wt.%)	Target type	Needle–target distance (cm)
DR1:ES-F	1	–	Fixed	10
				12
DR2:ES-X	2	–	Fixed	10
				12
				14
				16
				18
			Rotating	10
				12
				14
GNP/DR2:ES-X	2	1	Fixed	14
				16
				18
			Rotating	14
				16
				18

ES = electrospinning.
X = F or R if the fixed or rotating collector was used, respectively.

3. Results and discussion

3.1. Characterization of dry rubber

The dry rubber used for the preparation of the solutions/suspensions was characterized by XRD analysis, thermal analysis and ATR-IR spectroscopy, before and after the acetone treatment, in order to evaluate the preservation of the non-rubber components (such as proteins and phospholipids) in the treated DR. In fact, it is well known that the

Please cite this article as: I. Cacciotti, et al., Neat and GNPs loaded natural rubber fibers by electrospinning: Manufacturing and characterization, Materials and Design (2015), http://dx.doi.org/10.1016/j.matdes.2015.09.054

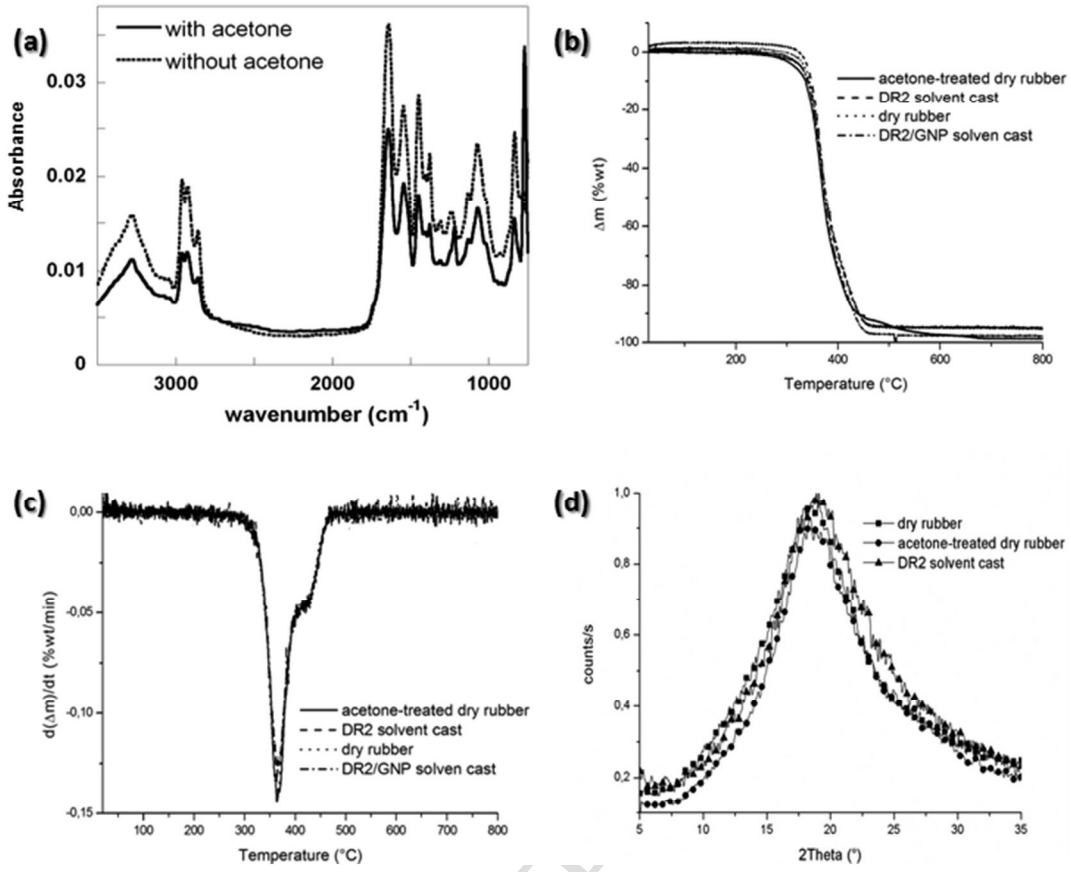

Fig. 1. (a) ATR-IR spectra of the dry rubber with (~~dotted~~ line) and without (~~continuous~~ line) acetone treatment. Spectra are staggered for clarity; (b) TG and (c) DTG curves of the dry rubber, acetone-treated dry rubber, neat and GNP loaded solvent cast DR2 films; (d) XRD diffraction pattern of the acetone treated and no-treated dry rubber and of the DR2 solvent cast film.

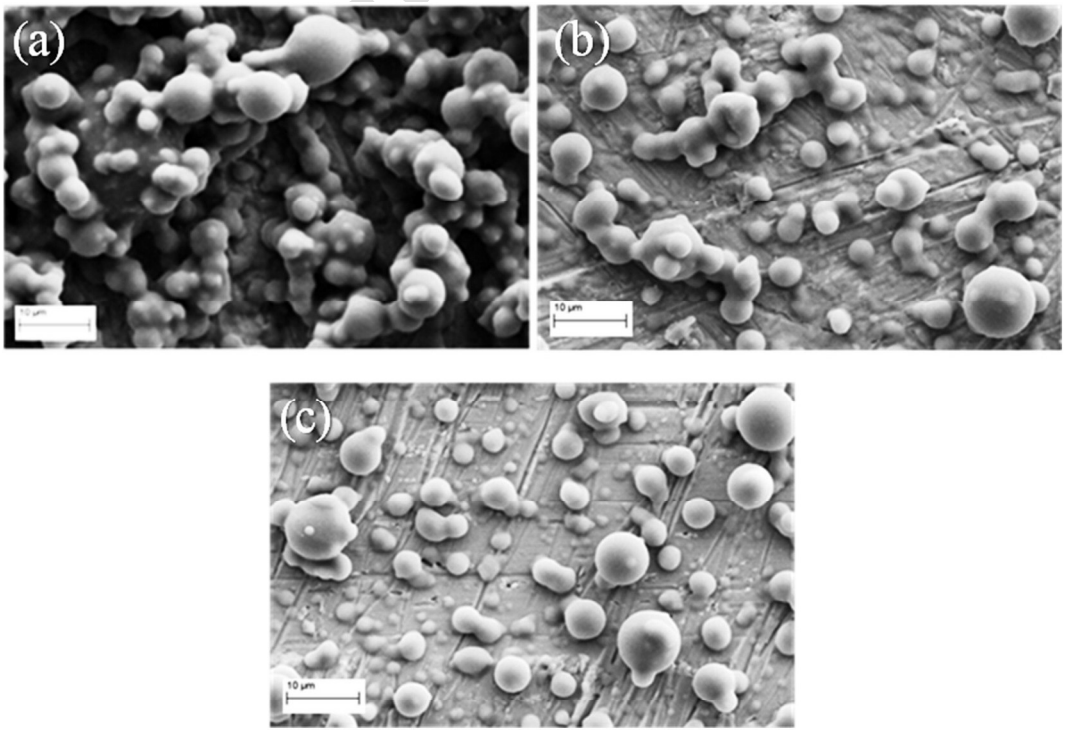

Fig. 2. SEM micrographs of the as received latex deposited at different needle–target distances (applied voltage 16 kV, feed rate 0,5 ml/h): (a) 10 cm, (b) 14 cm and (c) 16 cm.

Please cite this article as: I. Cacciotti, et al., Neat and GNPs loaded natural rubber fibers by electrospinning: Manufacturing and characterization, Materials and Design (2015), http://dx.doi.org/10.1016/j.matdes.2015.09.054

Table 2
Viscosity and conductivity values of the chloroform, as received latex and prepared solutions/suspensions.

Sample	Conductivity (μS/cm^2)	Viscosity (cP)		
		@ 20 rpm	@ 50 rpm	@ 100 rpm
Chloroform	0.011 ± 0.002	–	–	–
As received latex	7.2 ± 1.3	41.2 ± 0.1	30.6 ± 0.2	31.5 ± 0.2
DR1	0.011 ± 0.002	64.5 ± 0.7	61.0 ± 0.1	57.5 ± 0.7
DR2	0.008 ± 0.001	86.6 ± 0.1	76.7 ± 0.1	66.4 ± 0.3
GNP/DR2	0.013 ± 0.003	144 ± 1	116 ± 1	96.1 ± 0.2

presence of these components may enhance and promote the rubber crystallization [20]. Comparable ATR-IR spectra were acquired before and after the treatment of the latex (Fig. 1a), detecting the typical natural rubber functional groups [21] and the vibrational modes of the non-rubber components (i.e. proteins and phospholipids) at 1542 cm^{-1}, 1240 cm^{-1} and 1740 cm^{-1}, imputable to the N–H bending, the O–P–O asymmetric stretching and the C═O stretching of the phospholipids, respectively. Thus, it is possible to state that the acetone treatment did not influence and alter the presence of proteins and phospholipids. These results were confirmed by both thermogravimetric and X-ray diffraction analyses, proving that the selected treatment to obtain dry rubber was appropriate since all chemical characteristics of untreated rubber were maintained (Fig. 1b–d). Moreover it was verified through the same characterization techniques that the DR dissolution process in chloroform, in the case of the solutions prepared for the fiber preparation, did not induce any compositional modification. In details, in Fig. 1b–c the TG and DTG curves of the dry rubber samples with and without acetone treatment and of the neat and hybrid 2 wt.% DR solvent cast films are compared, presenting the same general shape. In all cases it is evident that the thermal degradation of the natural rubber is mostly a one-stage process [22], ranging the decomposition from approximately 300 °C to 450 °C with a mass loss of about 95%. The primary degradation peak in the DTG curves was ascribable to the thermal decomposition of the natural rubber into monomers, dimers and trimers, whereas the small shoulder curve at around 420 °C can be associated to the higher temperature degradation of crosslinked and cyclized networks [23]. XRD analysis of acetone treated and no-treated dry rubber and of the solvent cast film obtained from the chloroform solution showed the typical diffraction spectrum of this material in the amorphous phase, which is characterized by a broad peak at 2Θ 18° [24] (Fig. 1d). In fact, the isoprene molecules are coupled to form an irregular amorphous rubbery structure that cannot crystallize under normal conditions [25,26], but requires the application of a strain ("strain-induced crystallization", SIC). In conclusion, all the collected experimental data demonstrate that chloroform dissolution, as well as acetone treatment, did not induce any significant change to the rubber properties.

3.2. Morphology of the produced electrospun mats

The main technical issue was to find the optimum balance of solution/suspension viscosity and conductivity to allow the spinning of neat and GNP loaded NR solutions/suspensions. Based on the analysis and taking into account pure latex as reference, 2% *w/w* DR in chloroform and 1% w GNP with respect to DR were found to be a suitable combination in terms of conductivity and viscosity increase. The former was set up, testing different weight percentages in order to improve the spinning ability and fiber dimension control. SEM analysis confirmed the trend evidenced by Fong et al. [27] between viscosity and fiber quality: the processing is remarkably influenced by solution viscosity and for values below 60 cP spinnability is hindered. In fact, as received latex showed spraying behavior (Fig. 2), due to its low viscosity (i.e. 40 cP, Table 2), while increasing viscosity to 60 cP (i.e. DR1 solution) allowed fiber formation, although the fiber quality was very poor: fibers were not uniform, characterized by numerous and diffuse beads and imperfections, seemed to be melted together and tangled on each other (Fig. 3), owing to a not complete solvent evaporation during the flight from the needle orifice to the target. Furthermore, an increase of needle–target distances leaded to no spinnability. On the other hand, viscosity greater than 80 cP (DR2 solution) showed good spinnability

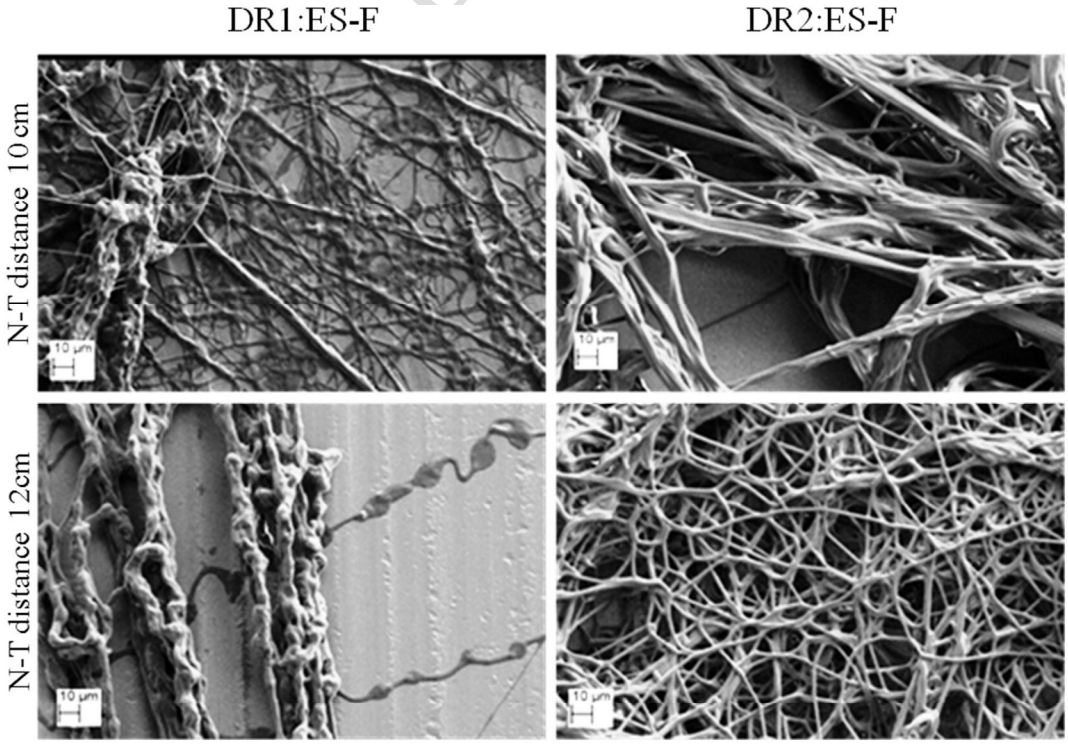

Fig. 3. SEM micrographs of the DR1:ES-F and DR2:ES-F fibers deposited at different needle–target (N–T) distances (applied voltage 16 kV, feed rate 0,5 ml/h).

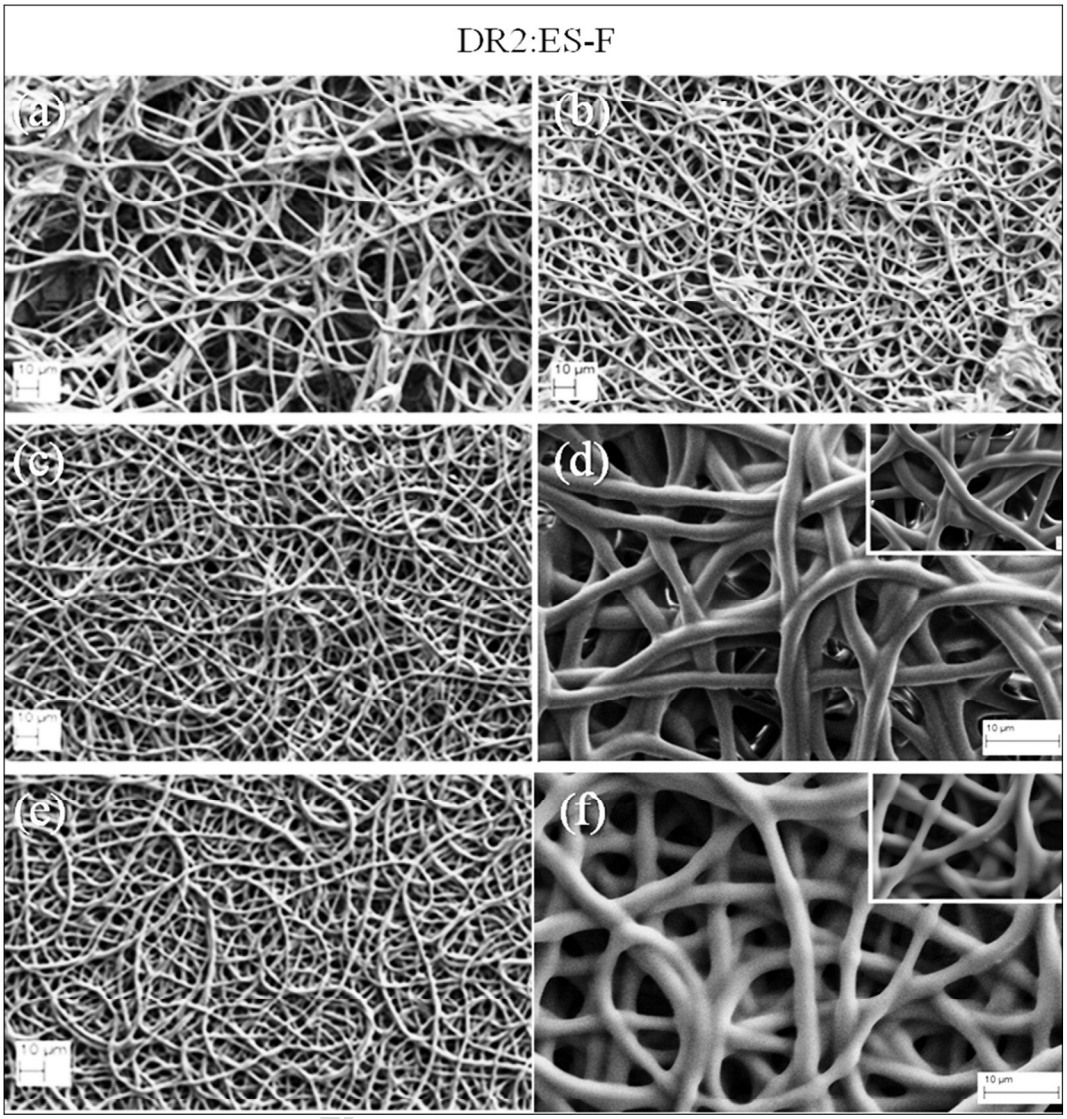

Fig. 4. SEM micrographs of the DR2:ES-F fibers deposited at different needle–target (N–T) distances (applied voltage 16 kV, feed rate 0,5 ml/h): (a) 12 cm, (b) 14 cm, (c–d) 16 cm, (e–f) 18 cm.

and uniform, homogeneous and defect-free fibers were obtained, independently from the needle-collector distance (Fig. 4). The best morphological characteristics were obtained selecting needle–target distances of 16 cm and 18 cm (Fig. 4). Indeed, increasing the needle–target distance allowed to obtain more uniform and homogeneous fibers, due to the better solvent evaporation and proper flight time. Moreover, high magnification micrographs reveal smooth surfaces without macroscopic defects (Fig. 4) and a reduction of fiber diameter increasing the needle–target distance (Table 3), in agreement with literature [27,28]. Fig. 5 shows a comparison between electrospun fibers from GNP/DR2 suspension at different needle–target distances (i.e. 14–18 cm). All the obtained GNP/DR2:ES-F samples consisted of uniform and bead-free fibers which were tangled on each other and showed some melted areas. This phenomenon seemed to decrease with increasing N–T distance. The high magnification SEM images evidenced a uniform dispersion and distribution of the filler within the fibers (Fig. 5). The maximum dimension of the filler was about 1 μm^2, whereas smaller aggregates were also observed. It is worth to notice that the hybrid GNP/DR fibers presented a rough surface, whereas the neat fibers were smooth. In a second step a rotating collector was employed in order to analyze the influence on fiber dimension and morphology and to try to induce polymer chains orientation. Concerning the fibers spun from the DR2 solutions on the rotating drum, the fiber quality is comparable to previous ones, in terms of both fiber dimension (Table 3) and surface roughness (Fig. 6), being all fibers very smooth. The DR2 fibers obtained varying the needle–target distance in the range 10–14 cm are compared in

Table 3
Average diameters of neat DR2 and hybrid GNP/DR2 electrospun fibers (all values are expressed as mean values ± standard deviation (SD)).

Sample	N–T distance (cm)	Fiber diameter (μm)
DR2:ES-F	10	1.5 ± 0.2
	12	1.4 ± 0.2
	14	1.1 ± 0.1
	16	1.0 ± 0.1
	18	0.9 ± 0.2
DR2:ES-R	10	1.2 ± 0.2
	12	1.1 ± 0.1
	14	1.1 ± 0.4
GNP/DR2:ES-F	14	1.3 ± 0.2
	16	1.3 ± 0.2
	18	1.2 ± 0.2
GNP/DR2:ES-R	14	1.3 ± 0.3
	16	1.1 ± 0.2
	18	1.2 ± 0.3

Please cite this article as: I. Cacciotti, et al., Neat and GNPs loaded natural rubber fibers by electrospinning: Manufacturing and characterization, Materials and Design (2015), http://dx.doi.org/10.1016/j.matdes.2015.09.054

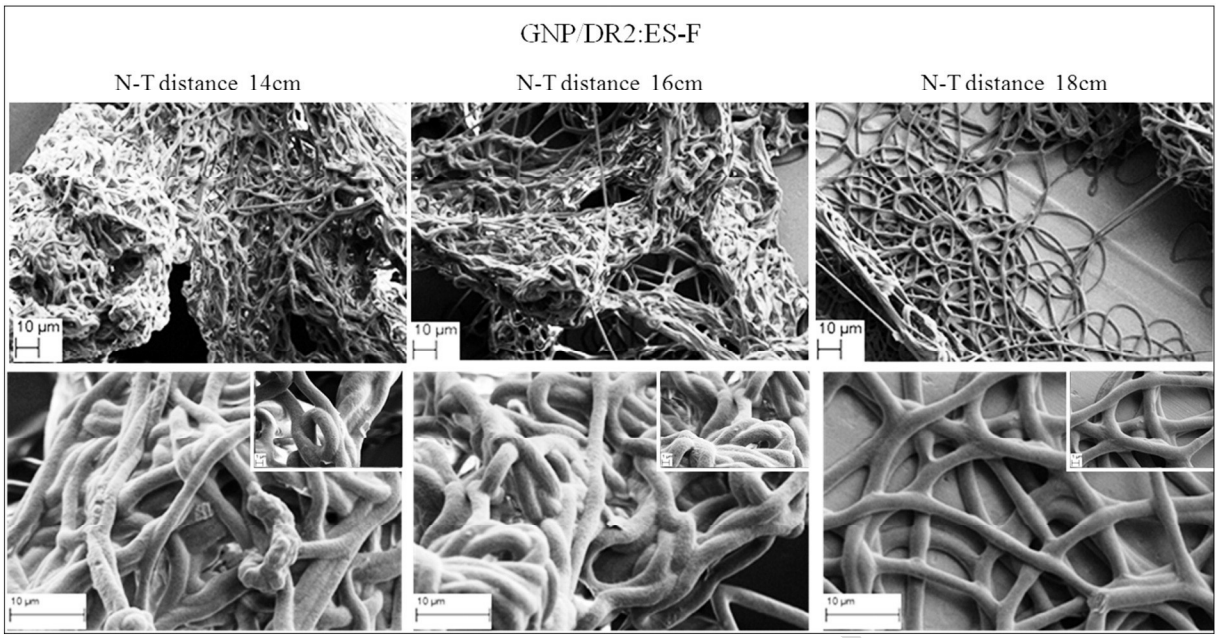

Fig. 5. SEM micrographs of the GNP/DR2:ES-F fibers deposited on a fixed collector at different needle–target (N–T) distances (i.e. 14 cm, 16 cm and 18 cm) (applied voltage 16 kV, feed rate 0,5 ml/h). In the inserts high magnification SEM micrographs are reported.

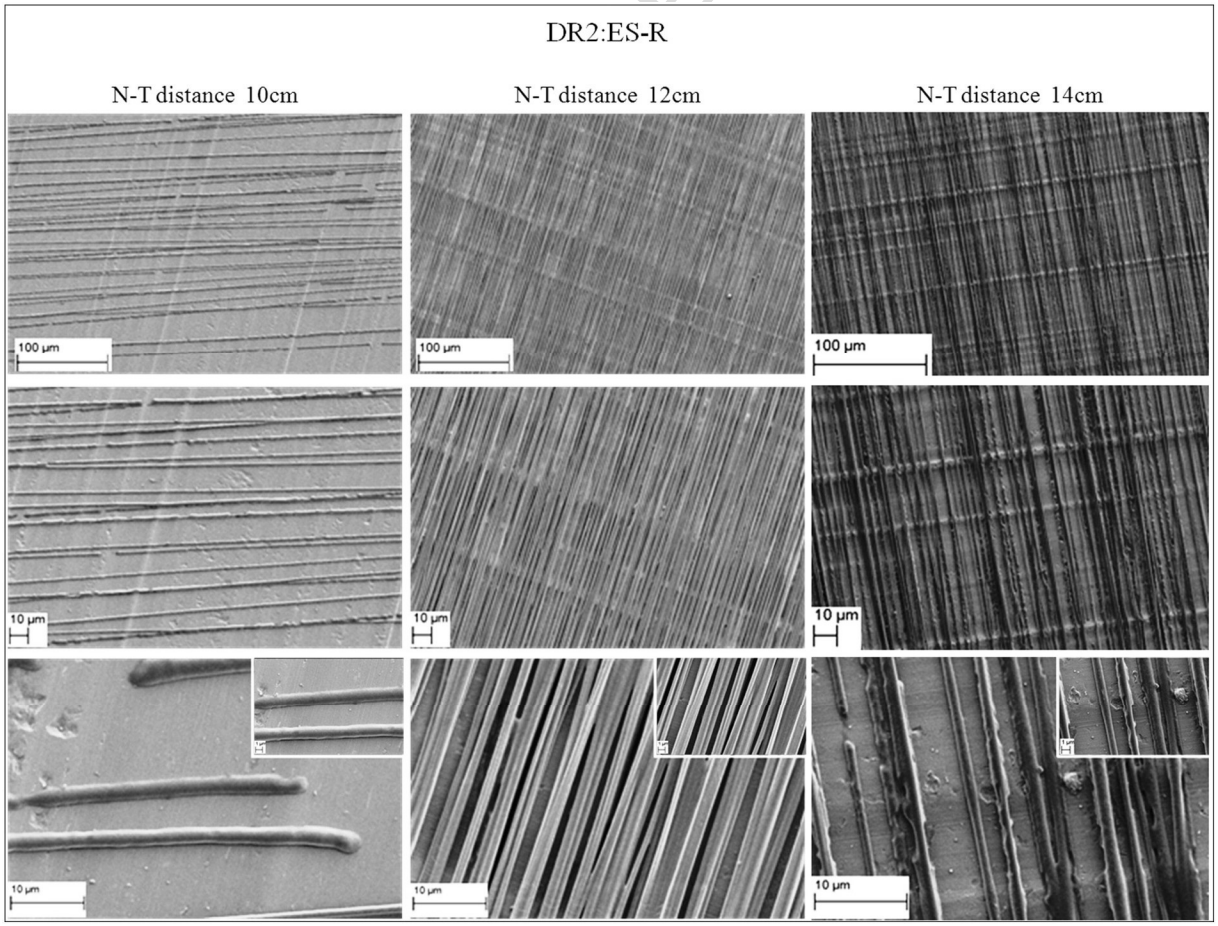

Fig. 6. SEM micrographs of the DR2:ES-R fibers deposited on a rotating collector at different needle–target (N–T) distances (i.e. 10 cm, 12 cm and 14 cm) (applied voltage 16 kV, feed rate 0,5 ml/h).

Please cite this article as: I. Cacciotti, et al., Neat and GNPs loaded natural rubber fibers by electrospinning: Manufacturing and characterization, Materials and Design (2015), http://dx.doi.org/10.1016/j.matdes.2015.09.054

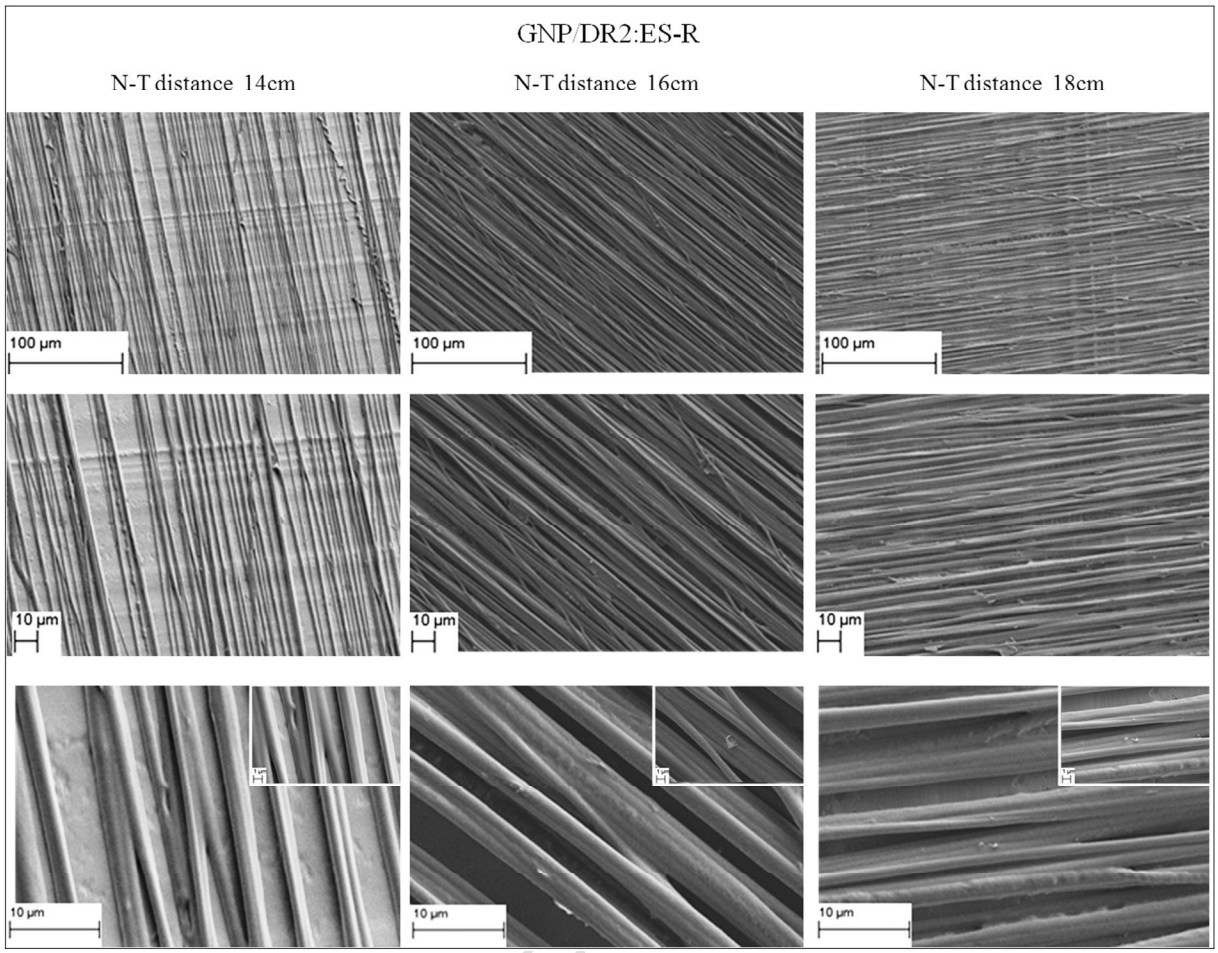

Fig. 7. SEM micrographs of the GNP/DR2:ES-R fibers deposited on a rotating collector at different needle–target (N–T) distances (i.e. 14 cm, 16 cm and 18 cm) (applied voltage 16 kV, feed rate 0,5 ml/h).

Fig. 6. The fibers deposited at a distance of 10 cm were uniform, smooth and bead-free, but spaced out and broken in many points and not perfectly aligned. In fact, since the elastomers/rubbers have glass transition temperatures lower than room temperature, the macromolecules chain segments are able to move and to rearrange their conformations in electrospun nanofibers. The molecular movement/relaxation usually occurs when the stretching force (particularly during the bending instability [28]) no longer exists, and is driven by entropy increase. Thus the breakage/conglutination of nanofibers can be observed with prolonging the storage time. This would be imputable to the characteristics of cis-1,4-polyisoprene, such as weak interaction between molecular chains, strong chain entanglement originating from rather flexible chain and elasticity, which may cause shrinking after release of Coulomb force [9]. On the contrary fibers spun at a distance of 12 cm were highly aligned, uniform, bead-free and did not present any type of morphological imperfection. The fibers deposited at a distance of 14 cm were very similar to the ones obtained at 10 cm, showing high alignment, but also poor uniformity and the presence of surface defects. Thus, the sample deposited at 12 cm presented the best morphological characteristics and was subjected to the other characterizations. Comparing the diameters of the fibers deposited on the fixed and rotating targets at the same needle-collector distance (Table 3), it is evident that the kind of target does not play a significant influence on the final fiber diameter. This experimental evidence could be due to the limited speed of the rotating collector. As a matter of fact, since the fibers are composed of an elastomer, if they were stressed with a significant rotational force, the rubbery material would have been stretched in the rotational direction causing shrinkage in the other directions. It cannot be excluded that a higher rotational speed would have promoted this effect. The analysis of GNP loaded aligned fiber reveals the absence of beads, while their alignment is influenced by the selected needle–target distance (Fig. 7). Indeed, the fibers spun at 14 cm distance were neither highly aligned nor very uniform and seemed melted together, as evident in the high magnification micrographs. On the other hand, selecting the distance at 16 cm and 18 cm induced an improvement of the alignment and avoided the occurrence of melting phenomena. However, the uniformity of these fibers was not excellent, especially at 18 cm, revealing some surface imperfections, as evident in the high magnification micrographs.

The presence of the filler was detected in the high magnification SEM micrographs, revealing that in some cases, it was oriented in the direction of the fiber (Fig. 7). This effect is due to the anisotropic conductivity properties of the GNPs, which are therefore oriented in the direction where the conduction is favored [2]. The reported diameter size values reveal a slight decrement of the fiber diameter with the N–T distance (Table 3). Furthermore, the collector type, fixed or rotating, did not exercise any significant influence on fiber diameter, obtaining comparable values under the same processing parameters. As mentioned previously this could be due to the limited rotating speed of the rotating drum. A comparison between the diameters of the fibers obtained spinning the DR2 solution and the GNP/DR2 suspension for N–T distances of 14 cm, 16 cm and 18 cm provided interesting results. Indeed, the hybrid fibers were slightly thicker than the related neat ones. This phenomenon is strictly correlated to the starting solution properties. As reported in literature, the solution properties, in terms of conductivity and viscosity, play contrasting effects on fiber final diameter. An increase in the conductivity of the solution brings to the

Please cite this article as: I. Cacciotti, et al., Neat and GNPs loaded natural rubber fibers by electrospinning: Manufacturing and characterization, Materials and Design (2015), http://dx.doi.org/10.1016/j.matdes.2015.09.054

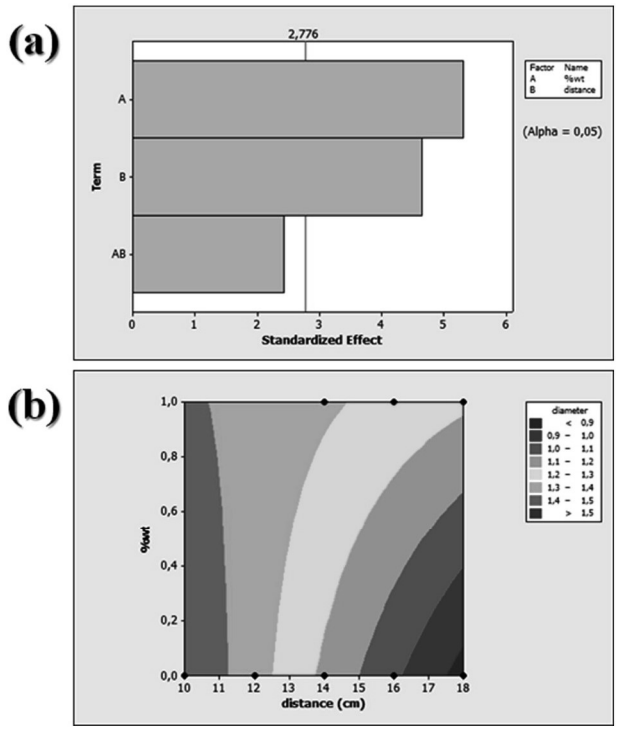

Fig. 8. (a) Pareto chart of standardized effect and (b) contour plot of the response surface related to the influence of the needle–target distance and the filler amount on the resultant fiber average diameter.

formation of thinner fibers, while an increment in the viscosity increases fibers final diameter [29–31].

The values of measured diameters suggest that, even if the addition of GNP to the DR2 solution increases both the conductivity and the viscosity, the increment of viscosity exercises a greater effect on fiber diameter than the increment of conductivity. Based on these results, we can state that viscosity is the main controlling factor of the electrospinning process since neat latex solutions showed spinnability even presenting low conductivity values, and GNP filled fibers were characterized by bigger diameter, despite higher conductivity of the related suspensions. Therefore, a semiempirical correlation between the major experimental parameters and the diameters of electrospun fibers was attempted. Based on literature [27] and experimental experience, two parameters were chosen as input data: one concerning the spinning solution/suspension (i.e. presence of filler which significantly alters the solution/suspension viscosity and conductivity) and the other the experimental set-up (needle–target distance). Experimental values of DR2 e DR2/GNP samples were used (Table 3). The best fitting mathematical model for the found experimental data is:

$$d = 0.63\ \text{wt.}\% + 0.080\ \text{distance} + 0.055 \cdot (\text{distance} \cdot \text{wt.}\%) + 2.3.$$

where 'd' is the fiber average diameter (expressed in μm), 'distance' the needle–target distance (expressed in cm), wt.% the filler amount in weight percentage. Considering the related Pareto chart (Fig. 8a) and contour plot of fiber average diameter in function of the two considered parameters (Fig. 8b), it is evident that both the filler amount (A) and the needle–target distance (B) can exercise significant effects on the average diameter of the produced fibers, with a confidence higher than 95%. On the other hand, the interaction factor (AB) does not statistically play a remarkable influence on the average diameter of the electrospun fibers, presenting a confidence of 95%.

The regression is in accordance with the physic of the process, since it can be assumed that increasing the distance between needle and target allows higher shrinkage of the fibers as well as the presence of the filler somehow hinders it.

3.3. Microstructural organization and orientation of polymeric chains

The electrospun mats were analyzed through XRD and ATR-IR in order to investigate the microstructural organization and orientation of the polymeric chains in the fibers. As regards XRD results, in all cases, a single broad peak at 18°, typical of the natural rubber, was detected and presented the characteristic shape of the amorphous NR (Fig. 9). Some authors [32] reported contradictory data, stating that the electrospinning process favors the crystallization in polymers with low T_g (≈−60 °C), such as polyesters. However, the acquired spectra showed no evidence of material crystallinity. It is possible to address the lack of crystallinity neither to the poor stretching after spinning nor to the low amount of dry rubber content in the spinning solution.

The preferential orientation of the polymeric chains in the produced samples was investigated by polarized infrared spectroscopy. The acquired polarized ATR-IR spectra were analyzed considering the peak at 2960 cm^{-1}, related to the CH_3 asymmetric stretching, as reference band, since its dichroic ratio is unitary, independently of the polymer's structure [18,19]. In our case, for all samples the dichroic ratios of the peaks at 1367 cm^{-1} and 837 cm^{-1} were calculated, since, as previously mentioned, these two peaks are assigned to the CH_3 deformation and the =CH out of plane bending of cis-1,4-polyisoprene, respectively. In fact, the =CH and the $-CH_3$ bonds lie in two almost perpendicular directions, and they strongly depend on the orientation of the polyisoprene units in the fibers and films [33].Table 4 summarizes the calculated dichroic ratios for the analyzed electrospun samples and the calculated dichroic ratios for the solvent cast films are reported, as a reference. As expected, for the cast film these values were approximately one for both peaks and in all configurations. Fig. 10a displays the ATR spectra in the 0° L and 90° L configurations. It is possible to notice that the relative intensities of the peaks are comparable. In fact, in the solvent casting technique no direct stress is applied for the formation of the samples and, consequently, the lack of an applied stress during the film formation leads to a random organization of the macromolecular chains in the sample. Concerning the electrospun samples, randomly oriented and aligned fibers showed different trends. The dichroic ratios of the randomly oriented fibrous mats were very similar to those of the solvent cast film. On the contrary, the aligned fibers presented high $R_L(0/90)$ and $R_T(0/90)$ values for the peak at 837 cm^{-1}, indicating a preferential orientation of the macromolecular chains. In Fig. 10b the peaks at 837 $cm^{-1}$of the ATR spectra in the $R_L(0/90)$ and $R_T(0/90)$ configurations are compared. The orientation was probably given by the processing technique itself and in particular by the ejection of the solution during the formation of the Taylor cone. It is highly unlikely that the force applied through the rotating drum could have induced the

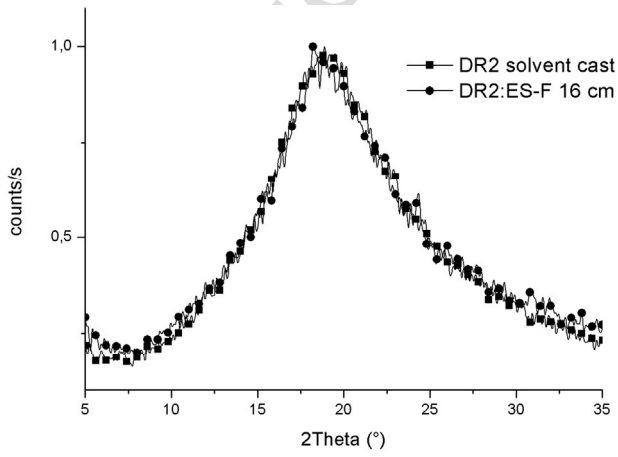

Fig. 9. Comparison of XRD spectra of DR2 solvent cast film and DR2:ES-F fiber mat.

Please cite this article as: I. Cacciotti, et al., Neat and GNPs loaded natural rubber fibers by electrospinning: Manufacturing and characterization, Materials and Design (2015), http://dx.doi.org/10.1016/j.matdes.2015.09.054

t4.1 **Table 4**
t4.2 Dichroic ratio values of the solvent cast and electrospun samples.

t4.3 Sample	R_L (0/90)		R_T (0/90)		R_0 (L/T)		R_{90} (L/T)	
t4.4	1370 cm^{-1}	837 cm^{-1}	1370 cm^{-1}	837 cm^{-1}	1370 cm^{-1}	837 cm^{-1}	1370 cm^{-1}	837 cm^{-1}
t4.5 Solvent cast	1.00	1.14	1.10	0.92	1.01	1.03	1.11	0.83
t4.6 DR2:ES-F	0.96	0.83	1.06	0.89	0.90	0.97	1.00	1.05
t4.7 DR2:ES-R	1.07	1.87	1.34	2.01	1.26	1.36	1.58	1.47

orientation of the polymer chains, being the collector's speed too slow. The alignment of the macromolecular chains was probably due to the influence of the electrostatic field on the polymer jet, which was able to create elongation strains and shear forces resulting in a high degree of molecular orientation. It was hypothesized that the polymer chains were oriented all in the same direction but are not packed to form a lattice. This reason could explain why the ATR measurements revealed a preferential orientation of the chains in the fiber, whereas the XRD spectra did not show diffraction peaks relative to a lattice organization.

4. Conclusions

Natural rubber based fibers were successfully manufactured by electrospinning, for the first time, starting from neat dry rubber solutions and GNPs/dry rubber suspensions. Different dry rubber solution concentrations were tested, in order to select the optimal one (i.e. 2 wt.%). For the hybrid systems, a disagglomeration procedure was developed to obtain a proper dispersion of the filler. Both randomly distributed and aligned fibers were produced using a fixed and rotating collector, respectively. The obtained fibers were uniform, homogeneous, defect-free and characterized by an average diameter of around 1 μm. Results clearly show that the solution/suspension viscosity can be considered the main controlling parameter in the electrospinning process, in terms of fiber dimension and quality, as expected and validated by a semiempirical equation. In the case of the hybrid fibers, the addition of the filler led to an increment in the suspension viscosity and conductivity. Consequently a slight increase in the fiber diameter (around 1.2 μm) was registered and this effect was accompanied by an evident roughening of the fiber surface. The internal fiber structure was also analyzed by X-ray diffraction and attenuated total reflectance experiments. The XRD diffraction patterns of the neat and hybrid spun fibers showed that the fibers are amorphous; however interesting results were obtained from the ATR-IR analysis, suggesting an influence of the electrospinning process on the molecular orientation of the natural rubber polymer chains. Indeed, significantly higher dichroic ratio values for the aligned fibers were obtained with respect to the randomly oriented ones, as well as to the solvent cast films. Thus the electrospinning process seemed to induce an orientation of the polymeric chains. Based on these findings, there is space for future works to promote strain induced crystallization, stretching the fibers during the spinning stage and using the oriented amorphous areas as nucleation sites.

Acknowledgements

The authors would like to thank Bridgestone Corporation for support and for permission to publish this work.

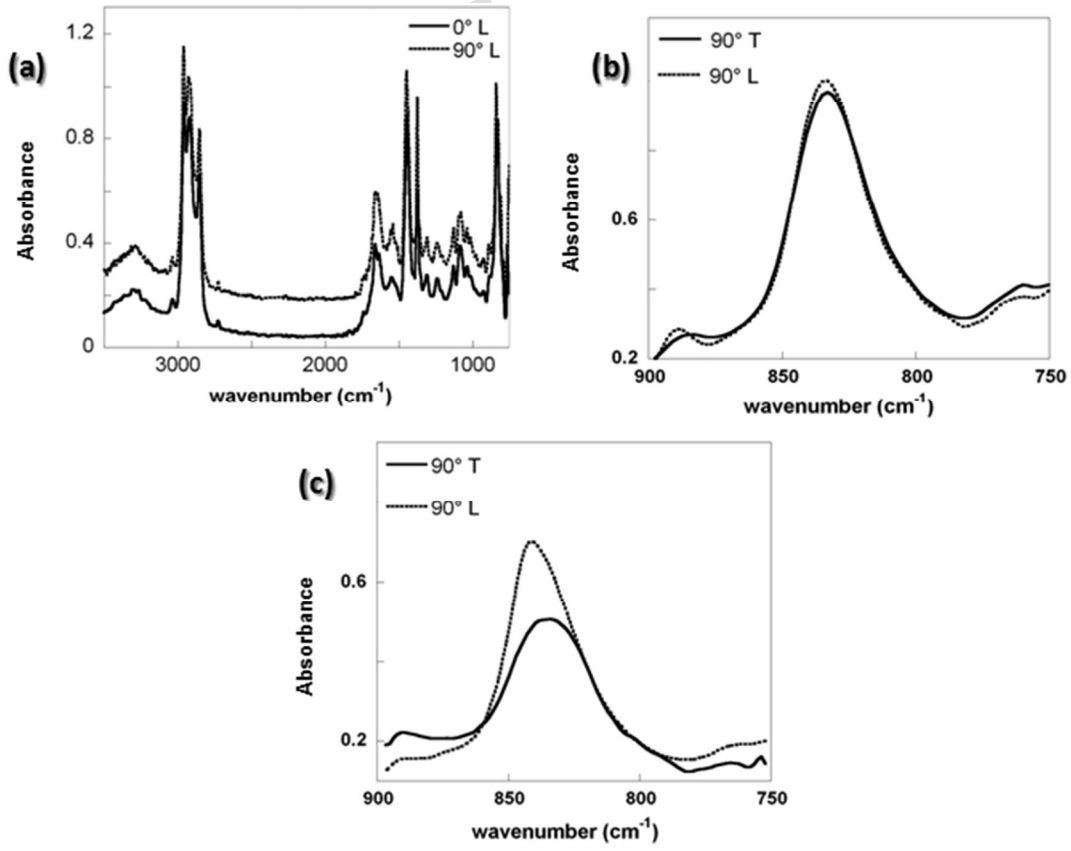

Fig. 10. (a) ATR spectra of the solvent cast film in the 0° L (continuous line) and 90° L (dotted line) configurations. ATR bands centered at 837 cm^{-1} obtained in the 90° L (dotted line) and 90° T (continuous line) configurations of random neat electrospun fibers (b); and aligned hybrid electrospun fibers (c). All spectra are normalized to the absorbance values at 2960 cm^{-1}.

Please cite this article as: I. Cacciotti, et al., Neat and GNPs loaded natural rubber fibers by electrospinning: Manufacturing and characterization, Materials and Design (2015), http://dx.doi.org/10.1016/j.matdes.2015.09.054

References

[1] S. Ramakrishna, K. Fujihara, W.-E. Teo (Eds.), An Introduction to Electrospinning and Nanofibers, World Scientific Publishing, Singapore, 2005.

[2] F.R. Lamastra, D. Puglia, M. Monti, A. Vella, L. Peponi, J.M. Kenny, F. Nanni, Poly(ε-caprolactone) reinforced with fibres of poly(methyl methacrylate) loaded with multiwall carbon nanotubes or graphene nanoplatelets, Chem. Eng. J. 195-196 (2012) 140–148.

[3] I. Cacciotti, A. Bianco, G. Pezzotti, G. Gusmano, Synthesis, thermal behaviour and luminescent properties of rare earth-doped titania nanofibers, Chem. Eng. J. 166 (2) (2011) 751–764.

[4] F. Nanni, F.R. Lamastra, F. Pisa, G. Gusmano, Synthesis and characterization of poly (e-caprolactone) reinforced with aligned hybrid electrospun PMMA/nano-Al_2O_3 fibre mats by film stacking, J. Mater. Sci. 46 (2011) 6124–6130.

[5] I. Cacciotti, E. Fortunati, D. Puglia, J.M. Kenny, F. Nanni, Effect of silver nanoparticles and cellulose nanocrystals on electrospun poly(lactic) acid mats: morphology, thermal properties and mechanical behaviour, Carbohydr. Polym. 103 (2014) 22–31.

[6] R. Dersch, T. Liu, A.K. Schaper, A. Greiner, J.H. Wendorff, Electrospun nanofibers: internal structure and intrinsic orientation, J. Polym. Sci. Part A: Polym. Chem. 41 (4) (2003) 545–553.

[7] M. Tian, Q.H. Hu, H.Y. Wu, L.F. Zhang, H. Fong, L.Q. Zhang, Formation and morphological stability of polybutadiene rubber fibers prepared through combination of electrospinning and in-situ photo-crosslinking, Mater. Lett. 65 (2011) 3076–3079.

[8] Q. Hu, H. Wu, L. Zhang, H. Fong, M. Tian, Rubber composite fibers containing silver nanoparticles prepared by electrospinning and in-situ chemical crosslinking, Express Polym. Lett. 6 (2012) 258–265.

[9] X. Hao, C. Bai, Y. Huang, J. Bi, C. Zhang, H. Cai, X. Zhang, L. Du, Preparation of cis-1,4-polyisoprene electrospun microfibers, Macromol. Mater. Eng. 295 (2010) 305–309.

[10] S. Sithornkul, P. Threepopnatkul, Control of mechanical properties and permeability of electrospun natural rubber with different composite systems, Adv. Mater. Res. 93-94 (2010) 619–622.

[11] L.M.M. Costa, L.H.C. Mattoso, M. Ferreira, Electrospinning of PCL/natural rubber blends, J. Mater. Sci. 48 (2013) 8501–8508.

[12] K. Cornish, Similarities and differences in rubber biochemistry among plant species, Phytochemistry 57 (2001) 1123–1134.

[13] H. Mooibroek, K. Cornish, Alternative sources of natural rubber, Appl. Microbiol. Biotechnol. 53 (2000) 355–365.

[14] J.M. Hagel, E.C. Yeung, P.J. Facchini, Got milk? The secret life of laticifers, Trends Plant Sci. 13 (2008) 631–639.

[15] M. Knite, V. Tupureina, A. Fuith, J. Zavickis, V. Teteris, Polyisoprene—multi-wall carbon nanotube composites for sensing strain, Mater. Sci. Eng. C 27 (2007) 1125–1128.

[16] W. Thongruang, C. Ritthichaiwong, P. Bunnaul, P. Smithmaitrie, K. Chetpattananondh, Electrical and mechanical properties of ternary composites from natural rubber and conductive fillers, Songklanakarin Journal of Science and Technology 30 (3) (2008) 361–366.

[17] N.J. Everall, A. Bibby, Improvements in the use of attenuated total-reflection fourier-transform infrared dichroism for measuring surface orientation in polymers, Appl. Spectrosc. 51 (8) (1997) 1083–1091.

[18] K.S. Abdulov, Calculation of the intensity and dichroism of the IR absorption bands of oriented polymers, J. Appl. Spectrosc. 72 (1) (2005) 138–141.

[19] K.S. Abdulov, Simulation of the influence of the polymer conformation, orientation, crystallinity, and stretching on its IR absorption spectrum, J. Appl. Spectrosc. 72 (6) (2005) 796–803.

[20] D.J. Siler, K. Cornish, Measurement of protein in natural rubber latex, Anal. Biochem. 229 (1995) 278–281.

[21] W. Pichayakorn, J. Suksaeree, P. Boonme, W. Taweepreda, G.C. Ritthidej, Preparation of deproteinized natural rubber latex and properties of films formed by itself and several adhesive polymer blends, Ind. Eng. Chem. Res. 51 (2012) 13393–13404.

[22] L.C.S. de Oliveira, E.J. de Arruda, R.B. da Costa, P.S. Gonçalves, A. Delben, Evaluation of latex from five Hevea clones grown in São Paulo State, Brazil, Thermochim. Acta 398 (2003) 259–263.

[23] A.K. Sircar, Characterization of isomeric elastomers using thermal analysis, J. Therm. Anal. 49 (1997) 293–301.

[24] M. Baboo, M. Dixit, K. Sharma, N.S. Saxena, Mechanical and thermal characterization of cis-polyisoprene and trans-polyisoprene blends, Polym. Bull. 66 (5) (2011) 661–672.

[25] H.M. Nor, J.R. Ebdon, Telechelic liquid natural rubber: a review, Prog. Polym. Sci. 23 (1998) 143–177.

[26] H. Kang, Y. Soo Kim, G.C. Chung, Characterization of natural rubber biosynthesis in *Ficus benghalensis*, Plant Physiol. Biochem. 38 (2000) 979–987.

[27] H. Fong, D.H. Reneker, Elastomeric nanofibers of SBS triblock copolymer, J. Polym. Sci. Polym. Phys. Ed. 37 (1999) 3488–3493.

[28] D.H. Reneker, A.L. Yarin, H. Fong, S. Koombhongse, Bending instability of electrically charged liquid jets of polymer solutions in electrospinning, J. Appl. Phys. 87 (9) (2000) 4531–4547.

[29] Z.M. Huang, Y.Z. Zhang, M. Kotaki, S. Ramakrishna, A review on polymer nanofibers by electrospinning and their applications in nanocomposites, Compos. Sci. Technol. 63 (2003) 2223–2253.

[30] A. Bianco, E. Di Federico, I. Cacciotti, Electrospun poly(ε-caprolactone)-based composites using synthesized β-tricalcium phosphate, Polym. Adv. Technol. 22 (12) (2011) 1832–1841.

[31] I. Cacciotti, M. Calderone, A. Bianco, Tailoring the properties of electrospun PHBV mats: co-solution blending and selective removal of PEO, Eur. Polym. J. 49 (2013) 3210–3222.

[32] D.H. Reneker, W. Kataphinan, A. Theron, E. Zussman, A.L. Yarin, Nanofiber garlands of polycaprolactone by electrospinning, Polymer 43 (2002) 6785–6794.

[33] B. Amram, L. Bokobza, J.P. Queslel, L. Monnerie, Fourier-transform infra-red dichroism study of molecular orientation in synthetic high cis-1,4-polyisoprene and in natural rubber, Polymer 27 (1986) 877–882.

Please cite this article as: I. Cacciotti, et al., Neat and GNPs loaded natural rubber fibers by electrospinning: Manufacturing and characterization, Materials and Design (2015), http://dx.doi.org/10.1016/j.matdes.2015.09.054